Thermoacoustic Instability in Two-Dimensional Fluid Complex Plasmas

Nikita P. Kryuchkov,[1] Egor V. Yakovlev,[1] Evgeny A. Gorbunov,[1] Lenaic Couëdel,[2,3]
Andrey M. Lipaev,[4] and Stanislav O. Yurchenko[1,*]

[1]*Bauman Moscow State Technical University, 2nd Baumanskaya street 5/1, 105005 Moscow, Russia*
[2]*CNRS, Aix Marseille Université, PIIM, UMR 7345–F-13397 Marseille, France*
[3]*Physics and Engineering Physics Department, University of Saskatchewan, 116 Science Place, S7N 5E2 Saskatoon, Canada*
[4]*Joint Institute for High Temperatures, 125412 Moscow, Russia*

(Received 9 April 2018; revised manuscript received 19 June 2018; published 17 August 2018)

Thermoacoustic instability in a fluid monolayer complex plasma is studied for the first time. Experiments, theory, and simulations demonstrate that nonreciprocal effective interactions between particles (mediated by plasma flows) provide positive thermal feedback leading to acoustic sound amplification. The form of the generated sound spectra obtained both in experiments and simulations excellently agrees with theory, justifying thermoacoustic instability in the fluid complex plasma. The results indicate a physical analogy between collective fluctuation dynamics in reactive media and in systems with nonreciprocal effective interactions exposing an activation behavior.

DOI: 10.1103/PhysRevLett.121.075003

Introduction.—Thermoacoustics has a long history, dating back to Rayleigh [1,2], who noted that a gas heated synchronously with compression and cooled with rarefaction stimulates acoustic oscillations, which may result in *thermoacoustic instability* [3–5]. Thermoacoustic instability can provide a highly efficient transfer of chemical energy to acoustic oscillation energy during exothermic reactions, which is attractive for modern applications, e.g., in engines and combustion technologies [6–11]. From the fundamental point of view, thermoacoustic instability may cause pulsations at flame fronts, leading to their acceleration and change in the combustion regime in reactive media [12–15].

In addition to chemical systems, the activation dynamic behavior can arise in open systems with nonreciprocal effective interactions between particles, e.g., in two-dimensional (2D) complex (dusty) plasmas [16,17]. Complex plasmas are weakly ionized gases containing (negatively) charged microparticles. In the plasma of a capacitively coupled (CC) radio-frequency discharge, injected monodispersed spherical microparticles levitate above the electrode where the gravity is balanced by the electric forces and form a monolayer. Because of the vertical plasma flow which is focused downstream of each microparticle ("plasma wakes") [18–21], their effective interactions are nonreciprocal. In this nonequilibrium environment, the dynamics of the system is determined by the interplay between the energy source due to nonreciprocity and the dissipation due to neutral gas damping [22,23]. If the effects of nonreciprocity are weak, the system demonstrates effective Hamiltonian dynamics, which was employed to study generic phenomena in classical liquids and solids, e.g., melting and crystallization [24–29], diffusion [30,31], heat transfer [32,33], and plastic deformations [34–36]. Otherwise, nonreciprocal interactions can induce mode-coupling instability (MCI) in crystalline [37–41] and fluid [42,43] complex plasmas due to coupling between in- and out-of-plane modes, resulting in unstable hybrid modes. Developed MCI exhibits an activation thermal behavior, similarly to chemically reactive solids [41,44]. However, to the best of our knowledge, thermoacoustic instability has never been studied in complex plasmas.

In this Letter, we present the first study of thermoacoustic instability in a monolayer complex plasma fluid. Using experiments, molecular dynamics (MD) simulations, and theory, we demonstrate that nonreciprocal effective interactions between particles provide a positive thermal feedback, resulting in sound amplification. The profiles of the sound spectra obtained both in experiments and simulations remarkably agree with the theory, justifying thermoacoustic instability in fluid complex plasma. Our study proves a physical analogy between collective fluctuation dynamics in reactive media and in systems with nonreciprocal effective interactions exposing an activation behavior. The results open novel prospects in studies of collective dynamics in nonequilibrium and dissipative systems, spanning areas from combustion, thermochemistry, and chemical physics to multiagent systems, soft matter, and materials science.

Experimental study.—We conducted the experiments in a modified GEC cell filled with argon gas at 1.25 Pa in a CC rf glow discharge at 13.56 MHz and forward rf power 20 W. The technical details of the experiments were the same as in Ref. [41]. Melamine-formaldehyde microspheres with a diameter of (9.19 ± 0.14) μm and mass $m = 6.1 \times 10^{-10}$ g were injected in the discharge.

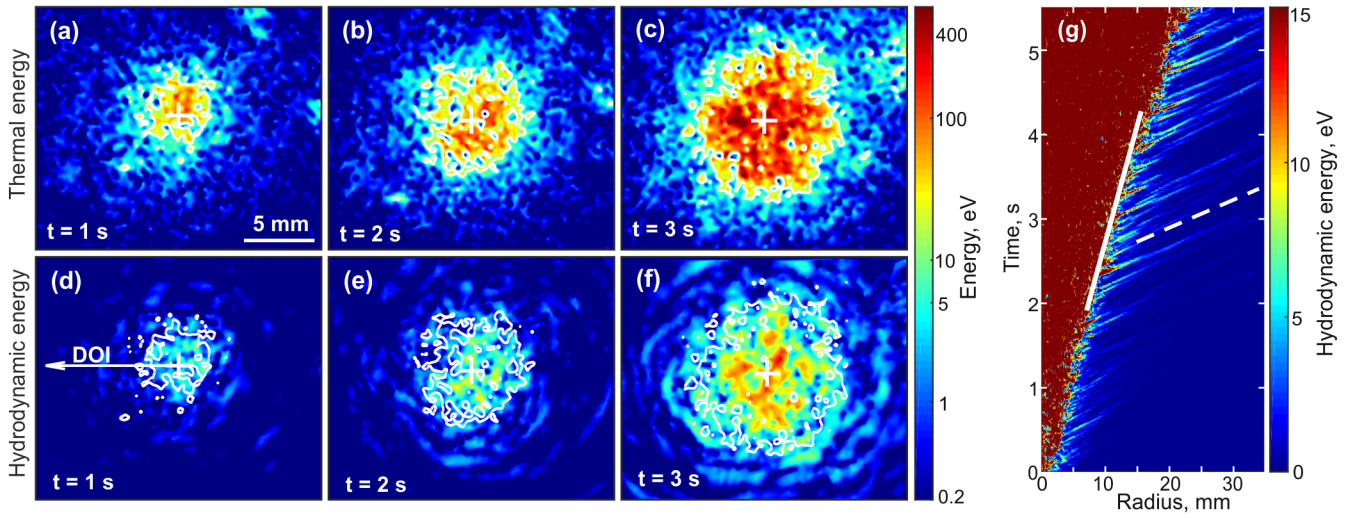

FIG. 1. Sound wave generation by the fluid complex (dusty) plasma: Evolution of the (a)–(c) thermal and (d)–(f) hydrodynamic energies of particles. The white contours in (a)–(f) mark the melted area where $T > T_m \simeq 12$ eV. (g) Evolution of the hydrodynamic energy in the radial direction of interest (DOI, coincides with the lattice principal direction) shown in panel (d). The white solid and dashed lines in panel (g) correspond to the flame front velocity, $v_{\rm fr} = 3.61 \pm 0.2$ mm/s, and longitudinal sound velocity, $C_L = 30 \pm 0.3$ mm/s, respectively. See also Video S1 [47].

The microparticles were illuminated by a laser sheet and the scattered light was recorded at a speed of 250 fps by a Photron FASTCAM SA6 camera fixed at the top of the chamber. The particles were then tracked using a standard approach [45,46]. An additional side-view camera Edmund Optics 0413M was used to verify that the microparticles formed a single layer. The sound generation was studied for the case where the plasma crystal "ignites" (in the densest region, where the growth rate of the crystalline MCI is the highest [37–40]) and the "flame front" expands radially outward [41]. To illustrate the sound generation by the fluid complex plasma, we calculated the thermal and hydrodynamic energies of particles using video images: $T = m\langle(\mathbf{v}_i - \langle\mathbf{v}_i\rangle)^2\rangle/2$, $K = m\langle\mathbf{v}_i\rangle^2/2$, where $\mathbf{v}_i$ is the instantaneous in-plane velocity of the ith particle and $\langle\cdots\rangle$ means the averaging over all the particles within the radius $2.4a$ around the ith particle, and $a = (390 \pm 20)$ μm is the mean interparticle distance between the neighboring particles in the crystal.

Figure 1 illustrates the evolution of the thermal energy (kinetic temperature) and hydrodynamic energy in our experiment. Figures 1(a)–1(c) show the expansion of the melted area (flame front propagation), similar to that observed in Ref. [41]. Figures 1(d)–1(f) clearly demonstrate that the flame front, propagating at a low velocity $v_{\rm fr} = 3.61 \pm 0.2$ mm/s, is accompanied by intense sound wave generation, as indicated by the radially diverging waves. The white contours in Figs. 1(a)–1(f) mark the areas where the temperature exceeds the melting temperature of crystal, $T > T_m \simeq 12$ eV (T_m is calculated from the crystal parameters, see details later in the Letter). The evolution of the hydrodynamic energy in the radial direction of interest [DOI, marked in Fig. 1(d)] is depicted in Fig. 1(g) and exposes the radially diverging waves released from the melted area. Therefore, our experiment reliably proves that the sound is generated by the fluid complex plasma and then propagates in the crystal.

Thermoacoustic instability.—To explain the mechanism responsible for the observed sound generation in fluid complex plasmas, we consider the equations [41,48]

$$\frac{\partial\rho}{\partial t} + \boldsymbol{\nabla}\cdot(\rho\mathbf{v}) = 0, \qquad \frac{\partial\mathbf{v}}{\partial t} + (\mathbf{v}\cdot\boldsymbol{\nabla})\mathbf{v} = -\frac{1}{\rho}\boldsymbol{\nabla}P - \nu\mathbf{v},$$
$$\frac{\partial T}{\partial t} + (\mathbf{v}\cdot\boldsymbol{\nabla})T = \chi\Delta T - \frac{2\nu}{C}(T - T_0) + q. \tag{1}$$

Here, $\rho = mn$ and n are the mass and number densities of particles, respectively; $\mathbf{v}$ is the hydrodynamic velocity; P is the pressure; ν is the damping rate (Epstein rate in case of complex plasmas, $\nu \simeq 1.5$ s^{-1} for our experimental conditions); T is the (kinetic) temperature of particles; χ is the thermal diffusivity; C is the heat capacity per particle (in 2D complex plasmas, $C \simeq 2$–3 due to the vertical motions of the layer); T_0 is the equilibrium temperature in absence of heating; $q = Q(n,T)/Cn$ is the heat source; and $Q(n,T)$ is the released power due to nonreciprocity of interactions.

We consider a compression wave propagating across the system. Let fluctuations of density, velocity, and temperature be small and proportional to $\exp(-i\omega t + i\mathbf{k}\cdot\mathbf{r}) + \text{c.c.}$, where ω and $\mathbf{k}$ are the (complex) frequency and wave vector, respectively. The linearization of (1) near the state $n = n_0$, $T = T_0$, $\mathbf{v} = \mathbf{0}$ yields the dispersion relation

$$[\omega(\omega + i\nu) - c^2k^2]\left[\omega + i\left(\chi k^2 + \frac{2\nu}{C} - q_T\right)\right] = i\epsilon k^2, \tag{2}$$

where $\epsilon = q_n P_T$, $P_T = m^{-1}(\partial P/\partial T)_0$, $q_n = (\partial q/\partial n)_0$, $q_T = (\partial q/\partial T)_0$, $c^2 = (\partial P/\partial \rho)_0$ is the squared sound velocity, and the subscript 0 denotes the calculation at $n = n_0, T = T_0$. The parameters q_T and q_n characterize the thermal feedback of the media to the temperature and density fluctuations. In fluid complex plasmas, $q = \gamma T/C$, where γ is the fluid MCI growth rate [42]

$$\gamma = \frac{\omega_p \tilde{q}}{2\omega_{cr}}\left(1 + \frac{\Omega_v^2}{\omega_p^2}\right)\exp\left[-\frac{h}{2\lambda}\left(1 + \frac{\Omega_v^2}{\omega_p^2}\right)\right], \qquad (3)$$

where $\omega_p = \sqrt{2\pi Q_d^2 n/m\lambda}$ is the 2D plasma frequency, λ is the Debye length, Q_d is the particle charge, Ω_v is the vertical confinement frequency, $\omega_{\rm cr}$ is the (crossing) frequency between the in- and out-of-plane modes, h and $\tilde{q}$ are the effective length of the wake and its dimensionless charge [47]. One can see that $q_{n,T} > 0$ in fluid complex plasmas, which is crucial for observed sound generation.

Consider an acoustic wave with $\omega \simeq ck + \delta\omega(k)$, where $\delta\omega(k)$ is a small perturbation caused by thermoacoustic interaction. Then, the increment of instability $\Gamma = \mathrm{Im}(\omega)$ is readily obtained from Eq. (2) as

$$\Gamma(k) \simeq -\frac{\nu}{2} + \frac{\epsilon}{2}\frac{k^2}{c^2k^2 + (\chi k^2 + 2\nu/C - q_T)^2}. \qquad (4)$$

According to Eq. (4), $\Gamma(k)$ can be positive at a small damping rate if $\epsilon > 0$ (or $q_n > 0$, since P_T is always positive), which means the amplification of the sound in the fluid.

Figure 1 clearly shows the strong sound waves (observed in the crystal) generated by the fluid complex plasma. Owing to the fluctuation-dissipation theorem [49], the generation spectrum corresponds to the positive part of $\Gamma(k)$ in the active media (fluid plasma in our case) and its form can be found as

$$\Gamma(k) \propto \log\left[I(k)/I_0(k)\right], \qquad (5)$$

where $I_0(k)$ and $I(k)$ are the fluctuation intensity spectra in the crystal before and during the sound generation, respectively. Since the long-wavelength sound freely propagates in the crystal from the fluid, we use the measurements in the crystal to obtain experimentally the positive part of $\Gamma(k)$, related to the thermoacoustic instability in the fluid.

To prove that the experimentally observed sound generation is caused by thermoacoustic instability, we analyzed our data. The experimental current fluctuation spectra in the plasma crystal were obtained by applying the Fourier transform to the particle velocities in the manner reported in Refs. [41,50]. To obtain dimensionless fluctuation currents, particle velocities were normalized to the thermal value $v_T = \sqrt{2T/m}$ in each frame (we used the current temperature T in the region of analysis) and the equivalent

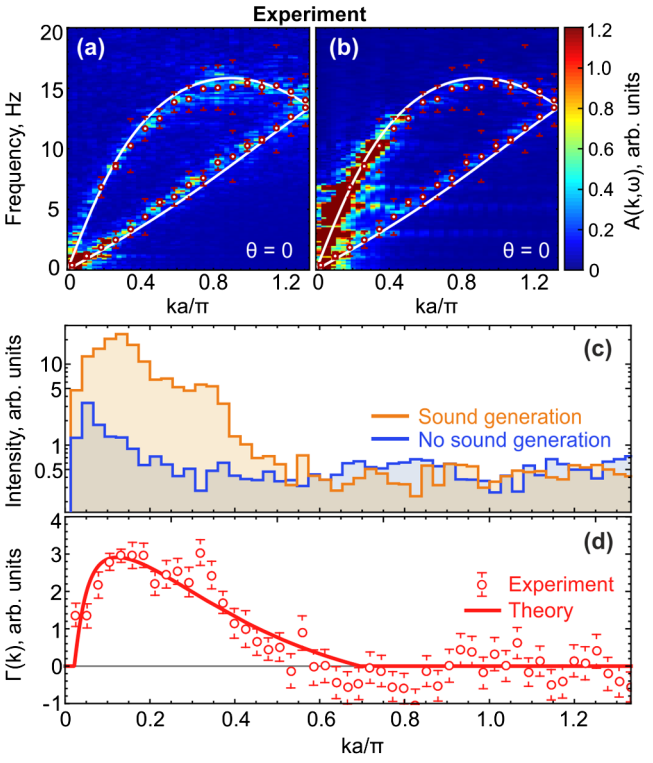

FIG. 2. Experimental evidence of thermoacoustic instability: Particle current fluctuation spectra (in principal direction) in the plasma crystal (a) before and (b) during sound generation from the melted area. (c) Intensities of fluctuation spectra $I(k)$. (d) Spectrum of thermoacoustically generated sound: experimental points with error bars compared with the theoretical fit by Eq. (4) shown by the red solid line.

number of frames was analyzed before the activation and during sound generation. The spectra were measured in the plasma crystal (with $T \simeq 0.1$–0.5 eV) at a distance of 23 mm from the center in the DOI shown in Fig. 1(d). The frequencies and damping rates depicted by symbols and bars in Figs. 2(a) and 2(b) were obtained by fitting of intensity spectra to two Lorentzians in the way reported in Refs. [50,51]. The white solid lines are fits by the theoretical dispersion relations [39,40] for a 2D system of particles interacting via the Debye-Hückel (Yukawa) potential $\varphi(r) = (Q_d^2/r)\exp(-r/\lambda)$ (since the effect of plasma wakes on phonon spectra is negligible in stable crystals far from the MCI [39]), which determines the screening parameter $\kappa = a_{\rm WZ}/\lambda = (\pi\lambda^2 n)^{-1/2}$ (where $a_{\rm WZ}$ is the Wigner-Seitz radius). We obtained the charge $Q_d = -(17 \pm 1.0) \times 10^3 e$, the screening parameter $\kappa = 1.15 \pm 0.1$, and the longitudinal and transversal acoustic velocities $C_L = (30.3 \pm 2.0)$ mm/s and $C_T = (6.6 \pm 0.4)$ mm/s, respectively. At these parameters, the plasma crystal melts at the temperature $T_m \simeq 12$ eV [52,53].

Using the density of fluctuation states $A(k,\omega)$ shown in Figs. 2(a) and 2(b), one can obtain the spectra $I(k)$ by integrating over frequencies, $I(k) = \int d\omega A(k,\omega)$; the

results are shown in Fig. 2(c). The spectrum $\Gamma(k)$ obtained using Eq. (5) is shown by symbols in Fig. 2(d). To compare the theoretical form of the spectrum (4) to experimental results, we calculated separately the thermal diffusivity χ. By fitting the theoretical self-similar profile for the temperature in the propagating flame front (as in Ref. [41]), we obtained the thermal diffusivity $\chi = (8.47 \pm 0.3)$ mm^2/s, which is in good agreement with Refs. [33,41]. Since χ changes slightly when the system undergoes melting [33], we used its value to fit (4) to experimental data using the least-square method. As a result, we obtained $c = (32.7 \pm 7.8)$ mm/s (which is close to C_L) and $q_T - 2\nu/C = (8.27 \pm 3.0)$ s^{-1}. The red solid line in Fig. 2(d) corresponds to the fitted positive part of Eq. (4). One can see excellent agreement between experimental and theoretical profiles of the sound generation spectra, revealing thermoacoustic instability in the fluid complex plasma.

MD simulations.—To further demonstrate that thermoacoustic instability observed in our experiments is due to the reactivity of the media provided by nonreciprocal interactions between particles owing to plasma wakes, we performed MD simulations using a simplified point-wake model [39,40,47]. The point-wake model is appropriate for complex plasma crystals, but becomes less adequate for fluids, when particles approach the plasma wakes of other particles [40,42]. However, this model exhibits a reactive temperature behavior and provides a good qualitative description of the effects caused by plasma wakes, such as the temperature profile of the propagating flame fronts [41]. The parameters of the point-wake model were chosen to reproduce the experimental fluctuation spectra shown in Fig. 2 and the self-similar profile of the propagating front of nonequilibrium melting [47]. We used the experimental values of the charge of particles Q_d and the screening parameter κ. The damping rate ν was tuned to reach agreement in the profile of the propagating front and its velocity [47]. Video S2 [47], according to our MD simulations, shows remarkably similar sound wave generation to Video S1.

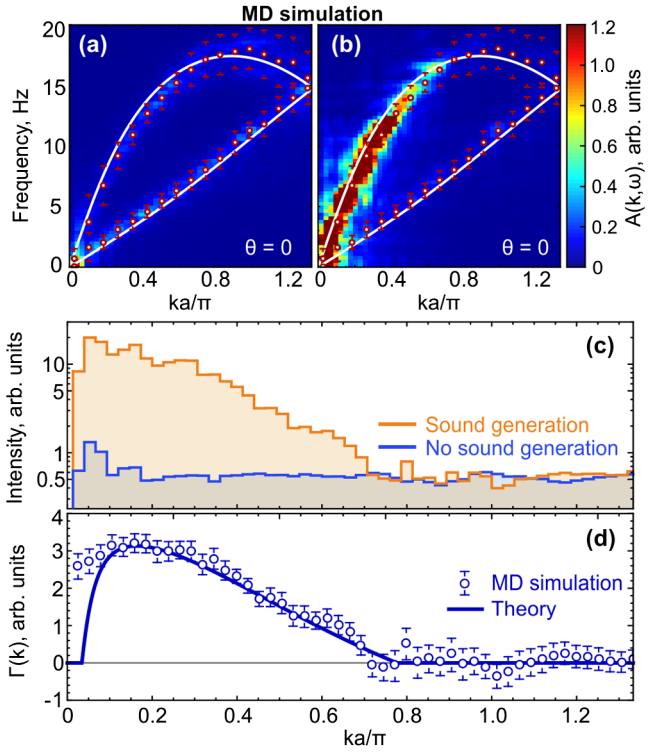

FIG. 3. Thermoacoustic instability revealed by MD simulations: Results of the MD simulation within the point-wake model [47]. The description is the same as in Fig. 2.

Our MD simulations were analyzed in the same manner as experimental data [47]. The results are shown in Fig. 3. Figures 3(a) and 3(b) present the fluctuation spectra before and during sound generation. The intensities of fluctuation spectra are shown in Fig. 3(c). Figure 3(d) clearly illustrates that the sound generation spectra obtained in MD simulations agree with the theoretical profile given by Eq. (4).

The discrepancies at $k \lesssim 0.1$ arise in Fig. 3(d), since the point-wake model provides an enhanced energy release [47] that shifts the region where $ck \gtrsim \delta\omega$ [54]. At intermediate wavelengths, one can see excellent agreement in Fig. 3(d). This result, in addition to our experimental findings shown in Fig. 2(d), clearly provides evidence of the thermoacoustic instability in 2D fluid complex plasmas.

Conclusions.—Although sound generation during nonequilibrium melting in plasma crystals was observed in previous studies [32,41], its physical mechanisms have never been understood and discussed. Similarly to melting, sound waves are generated during recrystallization, as it has been recently shown in [44]. Our study proves that the observed sound generation is due to thermoacoustic instability in the fluid complex plasma. Contrary to already known fluid and crystalline MCIs [37–43], thermoacoustic instability occurs in the long-wavelength range.

The mechanism responsible for the observed sound generation is related to the positive thermal feedback provided in our case by fluid MCI. However, one can expect that thermoacoustic instability can arise in a plasma crystal near the threshold of crystalline MCI, when the energy release power is close to the dissipation through Epstein damping. Related experimental studies of thermoacoustic instability in complex plasma crystals should be performed in the future.

An activation behavior is intrinsic to dissipative systems demonstrating bistability, e.g., driven-dissipative superfluids [55], open atomic many-body systems [56–59], dissipative photonic systems [60–62], and social (multiagent) systems [63–66]. In addition to chemical reactions, nonreciprocal systems, and open dissipative systems, positive thermal feedback necessary for thermoacoustic instability can arise at nonequilibrium phase transitions, e.g., at condensation during atmospheric phenomena [67,68]. For this reason, we expect that similar instabilities can occur in a broad range of open systems.

Our work reveals a remarkable physical analogy between fluctuations in chemical reactive media and systems with nonreciprocal interactions exposing an activation behavior. We believe that these results will stimulate theoretical and experimental studies in related areas of physics of nonequilibrium and dissipative systems, chemical physics, soft matter, and materials science.

The study was supported by Russian Science Foundation Grant No. 17-19-01691.

*st.yurchenko@mail.ru

[1] J. W. S. Rayleigh, Nature (London) **18**, 319 (1878).
[2] J. W. S. Rayleigh, *The Theory of Sound*, 2nd ed. (Dover, New York, 1945).
[3] F. Nicoud and T. Poinsot, Combust. Flame **142**, 153 (2005).
[4] X. Li, Y. Huang, D. Zhao, W. Yang, X. Yang, and H. Wen, Appl. Energy **199**, 217 (2017).
[5] G. Ghirardo, M. P. Juniper, and M. R. Bothien, Combust. Flame **187**, 165 (2018).
[6] K. McManus, T. Poinsot, and S. Candel, Prog. Energy Combust. Sci. **19**, 1 (1993).
[7] N. Syred, Prog. Energy Combust. Sci. **32**, 93 (2006).
[8] M. B. Toftegaard, J. Brix, P. A. Jensen, P. Glarborg, and A. D. Jensen, Prog. Energy Combust. Sci. **36**, 581 (2010).
[9] Y. Zhang and L. Huang, J. Sound Vib. **409**, 131 (2017).
[10] N. K. Mukherjee and V. Shrira, Combust. Flame **185**, 188 (2017).
[11] H. Zhao, G. Li, D. Zhao, Z. Zhang, D. Sun, W. Yang, S. Li, Z. Lu, and Y. Zheng, Appl. Energy **208**, 123 (2017).
[12] Y. B. Zeldovich, G. I. Barenblatt, V. B. Librovic, and G. M. Makhviladze, *The Mathematical Theory of Combustion and Explosion* (Consultants Bureau, New York, 1985).
[13] V. Alekseev, M. Kuznetsov, Y. Yankin, and S. Dorofeev, J. Loss Prev. Process Ind. **14**, 591 (2001).
[14] O. Peraldi, R. Knystautas, and J. Lee, Symp. (Int.) Combust. [Proc.] **21**, 1629 (1988).
[15] A. Kiverin, I. Yakovenko, and M. Ivanov, Int. J. Hydrogen Energy **41**, 22465 (2016).
[16] G. E. Morfill and A. V. Ivlev, Rev. Mod. Phys. **81**, 1353 (2009).
[17] A. Ivlev, H. Löwen, G. Morfill, and C. P. Royall, *Complex Plasmas and Colloidal Dispersions: Particle-Resolved Studies of Classical Liquids and Solids* (Word Scientific, Singapore, 2012).
[18] S. V. Vladimirov and M. Nambu, Phys. Rev. E **52**, R2172 (1995).
[19] M. Lampe, G. Joyce, G. Ganguli, and V. Gavrishchaka, Phys. Plasmas **7**, 3851 (2000).
[20] G. A. Hebner, M. E. Riley, and B. M. Marder, Phys. Rev. E **68**, 016403 (2003).
[21] R. Kompaneets, G. E. Morfill, and A. V. Ivlev, Phys. Rev. E **93**, 063201 (2016).
[22] A. V. Ivlev, J. Bartnick, M. Heinen, C.-R. Du, V. Nosenko, and H. Löwen, Phys. Rev. X **5**, 011035 (2015).
[23] N. P. Kryuchkov, A. V. Ivlev, and S. O. Yurchenko (to be published).
[24] V. A. Schweigert, I. V. Schweigert, A. Melzer, A. Homann, and A. Piel, Phys. Rev. Lett. **80**, 5345 (1998).
[25] C.-L. Chan, W.-Y. Woon, and L. I, Phys. Rev. Lett. **93**, 220602 (2004).
[26] A. Melzer, A. Homann, and A. Piel, Phys. Rev. E **53**, 2757 (1996).
[27] V. Nosenko, S. K. Zhdanov, A. V. Ivlev, C. A. Knapek, and G. E. Morfill, Phys. Rev. Lett. **103**, 015001 (2009).
[28] P. Hartmann, A. Douglass, J. C. Reyes, L. S. Matthews, T. W. Hyde, A. Kovács, and Z. Donkó, Phys. Rev. Lett. **105**, 115004 (2010).
[29] B. Smith, T. Hyde, L. Matthews, J. Reay, M. Cook, and J. Schmoke, Adv. Space Res. **41**, 1510 (2008).
[30] Y.-J. Lai and L. I, Phys. Rev. Lett. **89**, 155002 (2002).
[31] T. Ott and M. Bonitz, Phys. Rev. Lett. **103**, 195001 (2009).
[32] J. D. Williams, E. Thomas, L. Couëdel, A. V. Ivlev, S. K. Zhdanov, V. Nosenko, H. M. Thomas, and G. E. Morfill, Phys. Rev. E **86**, 046401 (2012).
[33] V. Nosenko, S. Zhdanov, A. V. Ivlev, G. Morfill, J. Goree, and A. Piel, Phys. Rev. Lett. **100**, 025003 (2008).
[34] V. Nosenko, S. Zhdanov, and G. Morfill, Phys. Rev. Lett. **99**, 025002 (2007).
[35] V. Nosenko, A. V. Ivlev, and G. E. Morfill, Phys. Rev. Lett. **108**, 135005 (2012).
[36] P. Hartmann, A. Z. Kovács, A. M. Douglass, J. C. Reyes, L. S. Matthews, and T. W. Hyde, Phys. Rev. Lett. **113**, 025002 (2014).
[37] A. V. Ivlev and G. Morfill, Phys. Rev. E **63**, 016409 (2000).
[38] L. Couëdel, V. Nosenko, A. V. Ivlev, S. K. Zhdanov, H. M. Thomas, and G. E. Morfill, Phys. Rev. Lett. **104**, 195001 (2010).
[39] S. K. Zhdanov, A. V. Ivlev, and G. E. Morfill, Phys. Plasmas **16**, 083706 (2009).
[40] L. Couëdel, S. K. Zhdanov, A. V. Ivlev, V. Nosenko, H. M. Thomas, and G. E. Morfill, Phys. Plasmas **18**, 083707 (2011).
[41] S. O. Yurchenko, E. V. Yakovlev, L. Couëdel, N. P. Kryuchkov, A. M. Lipaev, V. N. Naumkin, A. Y. Kislov, P. V. Ovcharov, K. I. Zaytsev, E. V. Vorob'ev, G. E. Morfill, and A. V. Ivlev, Phys. Rev. E **96**, 043201 (2017).
[42] A. V. Ivlev, S. K. Zhdanov, M. Lampe, and G. E. Morfill, Phys. Rev. Lett. **113**, 135002 (2014).
[43] T. B. Röcker, L. Couëdel, S. K. Zhdanov, V. Nosenko, A. V. Ivlev, H. M. Thomas, and G. E. Morfill, Europhys. Lett. **106**, 45001 (2014).
[44] L. Couëdel, V. Nosenko, M. Rubin-Zuzic, S. Zhdanov, Y. Elskens, T. Hall, and A. V. Ivlev, Phys. Rev. E **97**, 043206 (2018).
[45] S. S. Rogers, T. A. Waigh, X. Zhao, and J. R. Lu, Phys. Biol. **4**, 220 (2007).
[46] Y. Feng, J. Goree, and B. Liu, Rev. Sci. Instrum. **78**, 053704 (2007).
[47] See Supplemental Material at http://link.aps.org/supplemental/10.1103/PhysRevLett.121.075003 for experimental and MD video, as well as technical details of MD simulations.
[48] L. D. Landau and E. M. Lifshitz, *Fluid Mechanics*, 2nd ed. (Elsevier, Oxford, 1987), Vol. 6.

[49] L. D. Landau and E. M. Lifshitz, *Statistical Physics*, 3rd ed. (Elsevier, Oxford, 1980), Vol. 5.
[50] S. O. Yurchenko, K. A. Komarov, N. P. Kryuchkov, K. I. Zaytsev, and V. V. Brazhkin, J. Chem. Phys. **148**, 134508 (2018).
[51] S. A. Khrapak, N. P. Kryuchkov, and S. O. Yurchenko, Phys. Rev. E **97**, 022616 (2018).
[52] P. Hartmann, G. J. Kalman, Z. Donkó, and K. Kutasi, Phys. Rev. E **72**, 026409 (2005).
[53] N. P. Kryuchkov, S. A. Khrapak, and S. O. Yurchenko, J. Chem. Phys. **146**, 134702 (2017).
[54] The solution to Eq. (2) at $k = 0$ is $\omega = i(q_T - 2\nu/C)$. Then, from $|\mathrm{Im}(\omega)| \ll ck$ we obtain that Eq. (3) is suitable at $ka/\pi \gg (q_T - 2\nu/C)a/\pi c \simeq 0.034$ (for MD results) that agrees with Fig. 3(d). The same condition for the experimental results shown in Fig. 2(d) yields $ka/\pi \gg 0.032$.
[55] R. Labouvie, B. Santra, S. Heun, and H. Ott, Phys. Rev. Lett. **116**, 235302 (2016).
[56] S. Diehl, A. Micheli, A. Kantian, B. Kraus, H. P. Büchler, and P. Zoller, Nat. Phys. **4**, 878 (2008).
[57] D. Dast, D. Haag, H. Cartarius, J. Main, and G. Wunner, Phys. Rev. A **96**, 023625 (2017).
[58] S. Diehl, A. Tomadin, A. Micheli, R. Fazio, and P. Zoller, Phys. Rev. Lett. **105**, 015702 (2010).
[59] E. M. Kessler, G. Giedke, A. Imamoglu, S. F. Yelin, M. D. Lukin, and J. I. Cirac, Phys. Rev. A **86**, 012116 (2012).
[60] T. Mertz, I. Vasić, M. J. Hartmann, and W. Hofstetter, Phys. Rev. A **94**, 013809 (2016).
[61] S. R. K. Rodriguez, W. Casteels, F. Storme, N. Carlon Zambon, I. Sagnes, L. Le Gratiet, E. Galopin, A. Lemaître, A. Amo, C. Ciuti, and J. Bloch, Phys. Rev. Lett. **118**, 247402 (2017).
[62] J. Raftery, D. Sadri, S. Schmidt, H. E. Türeci, and A. A. Houck, Phys. Rev. X **4**, 031043 (2014).
[63] T. Vicsek and A. Zafeiris, Phys. Rep. **517**, 71 (2012).
[64] D. Helbing and P. Molnár, Phys. Rev. E **51**, 4282 (1995).
[65] M. Moussad, D. Helbing, and G. Theraulaz, Proc. Natl. Acad. Sci. U.S.A. **108**, 6884 (2011).
[66] I. Karamouzas, B. Skinner, and S. J. Guy, Phys. Rev. Lett. **113**, 238701 (2014).
[67] K. Naugolnykh and S. Rybak, J. Acoust. Soc. Am. **124**, 3410 (2008).
[68] K. Naugol'nykh, Acoust. Phys. **57**, 460 (2011).